Available at www.sciencedirect.com

ScienceDirect

journal homepage: www.elsevier.com/locate/he

Optimizing a steam-methane reformer for hydrogen production

M. de Jong[a], A.H.M.E. Reinders[a,*], J.B.W. Kok[b], G. Westendorp[c]

[a]Department of Design, Production and Management, Faculty of Engineering Technology, University of Twente, P.O. Box 217, 7500 AE Enschede, The Netherlands
[b]Department of Thermal Engineering, Faculty of Engineering Technology, University of Twente, P.O. Box 217, 7500 AE Enschede, The Netherlands
[c]HyGear B.V., Arnhem, The Netherlands

ARTICLE INFO

Article history:
Received 24 June 2008
Received in revised form
29 September 2008
Accepted 30 September 2008
Available online 22 November 2008

Keywords:
Reforming
Hydrogen production
Lumped parameter model
Natural gas

ABSTRACT

By means of steam reforming, natural gas is converted to carbon dioxide and hydrogen. The reactions take place in reactor tubes which are covered with catalyst at the inside, where the reactive mixture flows. At the outside they are heated by combustion of natural gas with air.

In this paper the conversion process is modeled for a single reactor tube by both chemical reaction models and heat transfer models. The model yields data of temperature, heat transfer and concentrations of hydrogen, carbon monoxide and natural gas along a reactor tube. Simulated temperatures have been validated with measured data from a prototype reformer. Next, the model was used to evaluate the performance of the reformer for six design modifications. It was found that the most promising improvements are created by increasing the air fraction in the burner and the thickness of the insulation shield.

1. Introduction

At present one of the most promising processes to generate hydrogen at distributed sites at reasonable costs is steam reforming on basis of natural gas by means of a reformer. This is a chemical device that converts natural gas to hydrogen by a chemical reaction with steam at pressures of 1.4–4.0 MPa and temperatures in the range 750–900 (°C). The mixture is heated and led over a catalyst bed, where it converts in an endothermic way to carbon monoxide and hydrogen. The heat necessary for this process is generated in a combustion chamber with a burner. In a next step the carbon monoxide reacts with steam to carbon dioxide and more hydrogen in the water/gas-shift reactor [1]. Downstream the water/gas-shift reactor, the product gas exists mainly of hydrogen, carbon dioxide, steam, and traces of methane and carbon monoxide. In a final step the hydrogen mixture is purified. This is done by the pressure swing adsorption process (PSA) [2]. The off-gas of the PSA is used as fuel in the above mentioned burner.

Multiple papers (see Refs. [2,3]) present a model of a non-adiabatic methane steam reformer membrane reactor (MSRMR) working in equilibrium conditions. The model was used to investigate the effects of some variables (e.g. temperature profile, separation efficiency, plant size) on the membrane area and the energy required by the process, which in turn affect fixed and operating costs. The simulations

* *Corresponding author*. Tel.: +31 53 4893681; fax: +31 53 4893631.
E-mail address: a.h.m.e.reinders@utwente.nl (A.H.M.E. Reinders).
0360-3199/$ – see front matter © 2008 International Association for Hydrogen Energy. Published by Elsevier Ltd. All rights reserved.
doi:10.1016/j.ijhydene.2008.09.084

Nomenclature

Acronyms

MSR	Methane Steam Reform
WGS	Water Gas Shift

Latin

A	Arrhenius pre-exponential factor
C_p	coefficient of heat capacity at constant pressure
D	tube diameter
E	activation energy
ΔG	mixture Gibbs free energy of formation (kJ kmol^{-1})
g	Gibbs free energy of formation of 1 species (kJ(kmol)$^{-1}$)
ΔH	heat of reaction (kJ kmol^{-1})
h	coefficient of heat transfer
K	chemical equilibrium constant
k	Arrhenius rate of chemical reaction
M	molar mass (kg kmol^{-1})
R	gas constant (kJ (K kg)$^{-1}$)
R_u	universal gas constant (kJ (K kmol)$^{-1}$)
r	reaction rate (kmol s^{-1})
T	temperature K or C
u	gas velocity (m s^{-1})
x	axial distance

Greek

π	number pie
υ	reaction vector
Φ	natural gas conversion efficiency

Subscripts and superscripts

i	number of reaction
in	gas flow in
f	flue gas
g	reactor gas
out	gas flow out
p	constant pressure
tube	reactor wall inside
wall	reactor wall

showed that the membrane area required sharply increases the reactor size and that for large plants the development of thin and permeable membranes is a key issue.

A program to compute the performance of a steam reformer is described in Ref. [4]. The results and accuracy are not discussed.

In Ref. [5] catalytic partial oxidation (CPO) reactions of methane in the presence of steam (low temperature CPO, LTCPO) over a noble metal catalyst were investigated. A quasi-homogeneous one-dimensional model was developed in order to model a lab-scale fixed-bed reactor to produce syngas. Predictions showed a reasonable comparison with experimental data on temperature profiles. The range of operational temperatures was, however, much lower than explored in the present paper.

The present paper uses similar modeling of the chemical reactions as in Refs. [2–5]. This paper focuses, however, on modeling of the limiting effects of, and interaction between, heat transfer and chemistry of methane steam reforming, rather than on maximum performance using a membrane.

Interesting work, with analytical methods applied similarly as in this paper on methane, was described with a focus on Diesel fuel steam reforming. In Ref. [6] the design and demonstration of an integrated steam reforming based hydrogen production unit using a Fischer–Tropsch diesel is reported. The system design is discussed in detail, including the fuel processor itself as well as the hydrogen purification and results from stand-alone operation of the combined unit operations is reported. The operation of the fuel-processing unit showed a fuel conversion of about 90%.

A thorough analysis of steam reforming, considering both equilibrium situations and deviations from this was presented in Ref. [7]. The analysis treats the chemistry at two levels: a global species balance assuming complete reaction and solution of the equilibrium composition at the specified reformer temperature. The global reaction allows for an energy balance that leads to analytical expressions for the thermal efficiency. Maximum efficiencies are determined in case of equilibrium. More realistic estimates of the efficiency are made while combining the chemical equilibrium solution with a system energy balance. The equilibrium solutions are compared to experimental measurements of the species and thermal efficiency of reforming diesel fuel, obtained with prototype compact steam reformers. The observed efficiency is significantly lower than the equilibrium prediction, indicating that both incomplete reaction and heat transfer losses reduce the performance. From this paper it is clear, that the challenge is to reach maximum conversion to hydrogen, as is indicated by the equilibrium situation. To reach this equilibrium condition, while avoiding very large reactors with large residence time, is the challenge. The present paper is targeted to provide a computational model, to support the design process of such a reformer. The reformer needs to be both small in size and to reach a conversion to hydrogen as close to equilibrium as possible. This paper models conversion of methane, while Refs. [6,7] model Diesel, hence quantitative comparisons are not possible.

This paper will focus on an analysis and optimization of the processes in the reformer reactor by means of a simulation model. First in Section 2 the design of a tubular reforming reactor will be explained. Subsequently the modeling of the chemical reactions in, and of the heat transfer to the reactor tubes, will be discussed in Section 3. The physical model represents the stationary operation of the reactor. In this model some design parameters are incorporated that can be used to optimize the design. The lumped parameter model and the solution procedure are described in Section 4. In Section 5 the parameter optimization will be presented. Finally in Section 6 options for the optimization of the reformer will be presented and quantified. The paper will be completed by conclusions in Section 7.

2. The tubular reactor design for a steam reformer

In Fig. 1 a schematic representation of a hydrogen production system on the basis of methane conversion is shown. It

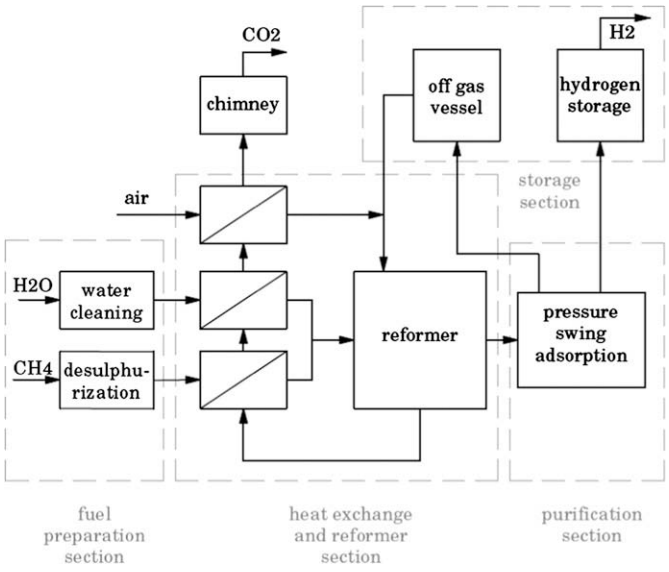

Fig. 1 – Scheme of a hydrogen production system comprising a steam-methane reformer.

consists of a reformer with multiple additional components for pre- and post-processing. Such a system is capable of producing 99.999% pure hydrogen out of methane.

The main task of the reformer is to convert a mixture of steam and methane into a hydrogen rich mixture. This is an endothermic catalyst reaction. The reformer section consists of a set of double walled reactor tubes filled with catalyst, a burner (to deliver and distribute the required heat) and a set of heat exchangers. The reactor tubes are enveloped by a flow guide tube.

3. Chemistry and heat transfer in a steam reformer tube

Crucial to the performance of the reformer is the design of the steam reformer tube, in which the reactants and the product gases flow. The flow guide enveloping the reformer tube has to be designed in such a way that it forces the hot flue gases to transfer heat to the reformer tube at the location, where the endothermic processes must take place. Inside the double walled reformer tube the chemical reactions occur, which convert the reactants natural gas and steam to hydrogen and inert product gases.

The reactants enter the reactor tube at the outside tube and flow to the tube end, reverse in direction and leave the reactor through the inner tube. The outside of the reactor tube is heated, in counter current exchange mode, by the hot flue gas passing between the flow guide and the reactor tube. Both the inner and outer tubes are filled with a porous catalyst structure. At the catalyst surface, the chemical reactions are initiated. Inside the reactor tubes two overall reactions occur: the Methane Steam Reform (MSR) reaction in Eq. (1) and the Water Gas Shift (WGS) reaction, as shown in Eq. (2):

$$CH_4 + H_2O \rightleftharpoons CO + 3H_2 \quad \Delta H_1 = 206\ \text{kJ mole}^{-1} \tag{1}$$

$$CO + H_2O \rightleftharpoons CO_2 + H_2 \quad \Delta H_2 = -41\ \text{kJ mole}^{-1} \tag{2}$$

The two global reactions here are identical to those used in several other papers, like Refs. [2–5]. Two types of catalysts are included to support these reactions: a platinum based catalyst for the MSR reaction (1) and another catalyst to support the WGS reaction (2). Since the MSR is endothermic, the platinum catalyst is located at the reactor tube inside walls. That way the catalyst heat loss due to the MSR reaction (1) is compensated by the heat conducted through the wall and supplied at the outside by the hot flue gas. The WGS reaction (2) is exothermic. For that reason the catalyst is placed at the interior flow domain of the reactor tube. These pieces of catalyst are clamped between the reactor tube walls. Flow guides are provided to prevent the mixture from reversed reforming at a lower temperature.

The reactions MSR and WGS are both equilibrium reactions and a global reaction can be expressed with a forward and a backward reaction rate. The rate at which the reactions occur depends on the distance to the equilibrium position (thermodynamics) and the speed at which the reactions occur (kinetics). The thermodynamic part of the chemistry is the ratio of the forward to the backward reaction speed. This ratio, which is temperature dependent, can be calculated by the distance to the equilibrium at which both reactions are equal in speed. The equilibrium constant for partial pressures (K_p) is used to this end. For the MSR reaction (Eq. (1)) and WGS reaction (Eq. (2)) the two following equilibrium constants as in Eqs. (3) and (4), respectively, can be formulated:

$$K_{p1}(T) = \frac{[CO][H_2]^3}{[CH_4][H_2O]} \tag{3}$$

$$K_{p2}(T) = \frac{[CO_2][H_2]}{[CO][H_2O]} \tag{4}$$

The value of each K_p as a function of temperature is calculated with the Van't Hoff Eq. (5):

$$K_p = K_{p,298}\exp\left(\frac{\Delta H}{R}\left[\frac{1}{298} - \frac{1}{T}\right]\right) \tag{5}$$

Here R is the gas constant that depends on gas mixture composition as given by Eq. (6):

$$R = \sum_{i=1}^{N} \frac{R_u}{y_i M_i} \tag{6}$$

The universal gas constant R_u is equal to 8.314 kJ/(kmol K). The term proportional to the reciprocal of T in Eq. (5) determines the equilibrium position. The reference value of the equilibrium constant $K_{p,298}$ is determined with the use of Eq. (7):

$$K_{p,i,298} = \exp\left(-\frac{\Delta G_i}{R298}\right) \tag{7}$$

The nominator in the exponent of Eq. (7) is the net change of the Gibbs free energy due to the forward and backward reactions in (1) and (2). This can be calculated with Eq. (8):

$$\Delta G_i = \sum_{j=1}^{N} \left(v_j^f - v_j^b\right) g_j \tag{8}$$

Here the v_j are the components of the forward and backward reaction vector and g_j are the Gibbs free energies of species j. These values for the species involved are given in Table 1. The equilibrium constant and hence the ratio between forward and backward reaction rates of both reactions (1) and (2) are now fully determined by Eqs. (3)–(8) and Table 1.

Now the rate of the reactions can be determined by specifying the rate $k_{f,i}$ of the forward reactions of the reactions (1) and (2). The rate $k_{b,i}$ of the backward reaction i is then found through Eq. (9) by:

$$k_{b,i} = \frac{k_{f,i}}{K_{p,i}} \tag{9}$$

The specific forward reaction rates of reactions (1) and (2) depend on temperature and are calculated with the Arrhenius Eq. (10):

$$k_{f,i}(T) = A_i \exp\left(-\frac{E_i}{RT}\right) \tag{10}$$

In which A_i is the pre-exponential factor and E_i is the activation energy [J kmol^{-1}]. The activation energy is determined empirically. It must be noticed that practical values may differ slightly, due to uncertainties in the catalyst characteristics. See also Refs. [8–10]. The values of the kinetic parameters in Eq. (10) used in this work are specified in Table 2. The reaction rates of reactions (1) and (2) are now found from:

$$r_i = k_{f,i}(T) \prod_{j=1}^{N} x_j^{v_j} \tag{11}$$

Table 1 – Gibbs free energy of formation of species involved in reaction

Substance	Formula	g_f^0
Hydrogen	H_2 (g)	0
Carbon monoxide	CO (g)	−137.150
Carbon dioxide	CO_2 (g)	−394.360
Water vapor	H_2O (g)	−228.590
Methane	CH_4 (g)	−50.790

Values valid at 25 °C and 1 atm (Ref. [9]).

Table 2 – Arrhenius kinetic parameters

Reaction number	Pre-exponential factor, A	Activation energy, E
(1)	4.225×10^{15}	240.1
(2)	1.955×10^{6}	67.13

4. A lumped parameter thermodynamic model

The lumped parameter thermodynamic model presented here, describes the heat transfer from the flue gas to the reactant gas in the reformer tubes and the chemical reactions taking place inside the reformer tubes. An important element in the model is the interaction between heat transfer and chemical reaction. The physical domain of the model is limited to the volume between the flow guide tubes and the reformer tubes, and the reformer tubes themselves. This numerical model is implemented in the computational computer program Matlab and is used to evaluate quantitatively modifications in the design. To obtain a model of the reactor space and the reactor tubes the physical situation is simplified. In Fig. 2, a layout of the simplified model is shown.

The heat transport in the reformer is simulated in one dimension for three different domains: the reactor space (volume between the flow guide tube and the reactor tube), the inside of the reactor tube and the reactor wall between the tube and reactor space. At the top the hot flue gas enters the domain. It leaves at $x = 0$ after transferring heat to the reactor wall.

$$\frac{dT_f}{dx} = \frac{1}{u\rho C_p} \pi D h_f \left(T_{wall} - T_f\right) \tag{12}$$

The gradient in temperature of the hot flue gas with axial distance is given by the differential Eq. (12) above. At the other side of the wall in counter flow the reaction mixture enters the

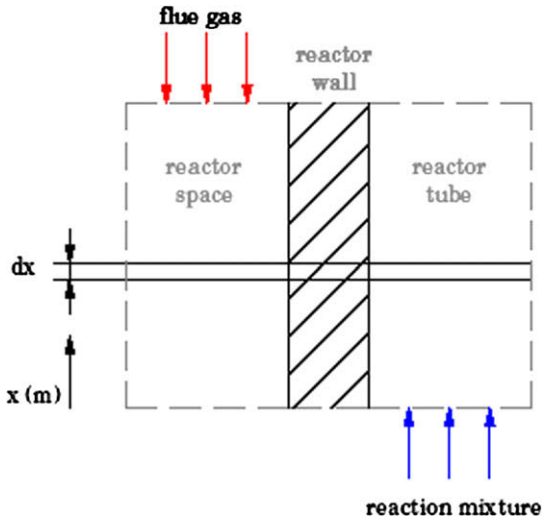

Fig. 2 – Physical domain of the model of the reactor chamber.

domain in the reformer tube at $x = 0$ and leaves at a high x value. This mixture is heated by the reactor wall and reactions that occur.

The MSR reaction (1) is endothermic, this reaction consumes heat. The WGS reaction is exothermic, which results in a heat production. The speeds at which the reactions occur, for the MSR and the WGS, are calculated at each location, using the Eqs. (3)–(10). The total amount of heat production is given for each reaction number (j) over flow area A times the reaction rate and heat of reaction j. When all model parts are assembled this leads to the differential equations for the gradient of the temperature of the reformer gas, the gradient of the CO concentration and the gradient of the wall temperature, respectively:

$$\frac{dT_g}{dx} = \frac{1}{u\rho C_p}\sum_{i=1}^{2}\left(\pi D h_g (T_{wall} - T_g) + \frac{1}{4}\pi D^2 \Delta H_i r_i\right) \quad (13)$$

$$\frac{d[CO]}{dx} = r_1 - r_2 \quad (14)$$

$$T_{wall} = \frac{h_f}{h_f + h_g} T_{flue} + \frac{h_g}{h_f + h_g} T_{tube} \quad (15)$$

The temperature of the wall is taken as the average temperature of both flue gas and reactor mixture times each heat transfer coefficient fraction. See for these equations also Refs. [11,12].

The heat transfer coefficients h_f and h_g need to be specified in order to close the Eqs. (12)–(15). For developed turbulent tube flows often the following Nusselt number correlations are used as an estimate for the heat transfer coefficient:

$$Nu = \frac{hD}{\lambda} = 0.0294 Re^{0.8} Pr^{0.8} \quad (16)$$

With a global velocity in and around the reformer tube of about 20 m s^{-1}, a diameter of 0.3 m and a gas temperature around 1200 °C, the Nusselt number can then be estimated to be about 100. With a conductivity coefficient of the gas of about 0.08 W/(m K) the heat transfer coefficients h_f and h_g can then be estimated to be about 30 W(K m^2) on basis of Eq. (16).

It can be expected, however, that these estimates are much too low, as much effort has been made to increase heat transfer above that of turbulent pipe flow. Inside the pipe the catalyst fins increase turbulence and boost heat transfer enormously. Outside the tube in the flue gas, also fins have been placed. For that reason in reality the heat transfer coefficients will probably be a magnitude higher, about 300–900. As the actual values have not been measured, the heat transfer parameters will be set here to match the experimental data. It was found that the best fit for h_g is 700 W/(K m^2) and h_f ranges from 500 to 950 W/(K m^2) depending on geometry. The used values are depicted in Fig. 3. To complete the validation these values would have to be verified in an additional non reacting flow experiment.

The set of ordinary differential equations is solved with boundary conditions at $x = 0$ for the reformer gas temperature and concentration, and for the hot flue gas temperature at large x. The set of ordinary differential equations was integrated with a Runge–Kutta method. As boundary conditions were imposed at both ends, a shooting method had to be applied. An estimated value was picked for the temperature at $x = 0$, at $x =$ large the calculated value for the temperature is compared with the calculated estimate and the initial value is corrected. Then the value of the temperature at $x = 0$ is

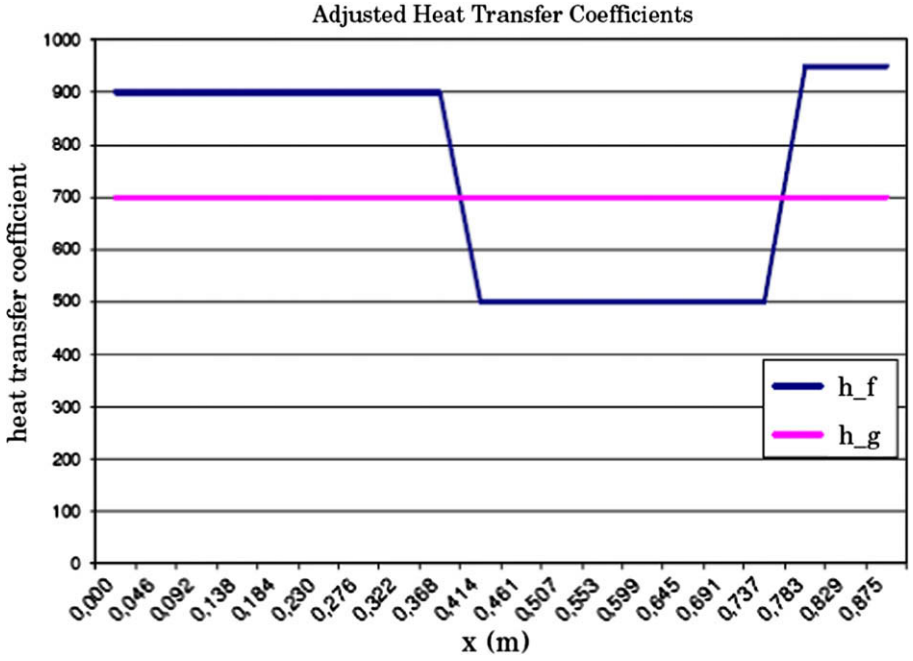

Fig. 3 – Employed heat transfer coefficients in model, h_f, between flue gas and outside reformer tube and, h_g, between reformer gas and inside reformer tube.

recalculated and again compared. This iteration is repeated till the difference is acceptable.

5. Simulation results and comparison with measurement data

An efficient lumped parameter thermodynamic model has been presented in Section 4. The qualitative behavior and accuracy will be discussed in this section. To this end a reference case was simulated and the results compared with measured data. In the measurements performed by HyGear on a reformer tube of their design, temperatures in the reformer were recorded during a period of 78 min after startup. The transient effects have already disappeared approximately 50 min after turning the system on. During this operation the methane flow was 60% of maximum capacity and the burner was fed with methane and regulated on a maximum wall temperature of 900 °C.[1]

The predicted and measured temperatures of the flue gas, reformer tube wall and the reformer gas are presented in Fig. 4 as a function of axial distance. The flue gas enters at 1300 K at $x = 0.9$ m and exits at $x = 0$ at 1000 K. The steam and natural gas mixture enter at $x = 0$ the reformer tubes and is reformed to CO and hydrogen when passing to the end of the reformer tube, where it exits the MSR process at 1000 K, after which it reverses to the WGS path in the inner tube. It can be observed that the measured wall temperatures fall well in between the predicted flue gas and reformer gas temperatures.

The predicted reactant and product concentrations are depicted in Fig. 5, as a function of axial distance. The methane concentration can be observed to decrease to 50% of its initial value, while Hydrogen and CO is produced, consuming steam in the process. About as much CO as CO_2 is produced. This can be explained by the WGS reactions which already participate in the process. Hence the CO_2 produced is not necessarily a loss. Unfortunately measured concentration data are not available for validation of these results.

6. Evaluation of the effect of design modifications

Next, the model has been used to evaluate the effect of design modifications on the performance of the reformer.

Nine design modifications were proposed:

1. an increase of the length of the reactor tubes;
2. an increase of the air factor in the burner fuel;
3. a change of the geometry of the holes in the outer reactor tube;
4. a change of the location of the holes in the outer reactor tube;

[1] Not applicable in this model but nevertheless important information following from the measurement results is that temperature differences between the tubes are significant, approximately 100 K. This effect is observed between the tubes. Because the model only simulates one tube, this fact is not included in the model.

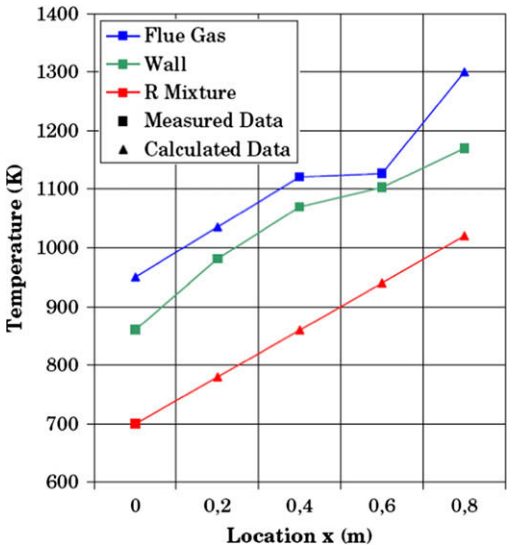

Fig. 4 – Comparison of measured and simulated temperatures in the reformer.

5. an increase of the steam factor in the reaction mixture;
6. a change of the reactor tube material;
7. modification of the design to create a variable reactor mixture speed;
8. a change of the size of the holes in the insulating shield; and
9. a change of the thickness of the insulating shield.

Modification 1–5 and 9 appeared to be suitable to be modeled in our analytical model and were therefore fit for further evaluation. Modifications 6–8 could not be modeled with the tool at our disposal and will not be discussed in the following sections.

Six design modifications are analyzed with our model. The effect of the modification on the performance of the reformer is expressed by the change of the efficiency of methane conversion due to the modification (see also Ref. [7]). This conversion efficiency of methane Φ_{CH4} is calculated by the following equation:

$$\Phi_{CH_4} = \frac{[CH_4]_{in} - [CH_4]_{out}}{[CH_4]_{in}}$$

The results are visualized in Fig. 6. From this figure it follows that the six design modifications proposed have indeed a positive effect on the methane conversion efficiency. Three modifications have a considerable effect, i.e. the extension of the reformer tubes, an increase of the air fraction in the burner and an increase of the thickness of the insulating shield. It is found that up to 12% more hydrogen can be produced by increasing the length of the reactor tubes by 50%, 9.5% more hydrogen can be produced by increasing the air fraction in the burner fuel by 50%, and by increasing the thickness of the insulating shield by 50%, 11% more hydrogen can be produced.

The results of the design modifications are comparable because the maximum tube temperature is similar for all cases, which is accomplished by decreasing the amount of fuel fed into the system. The results are explained by two major effects.

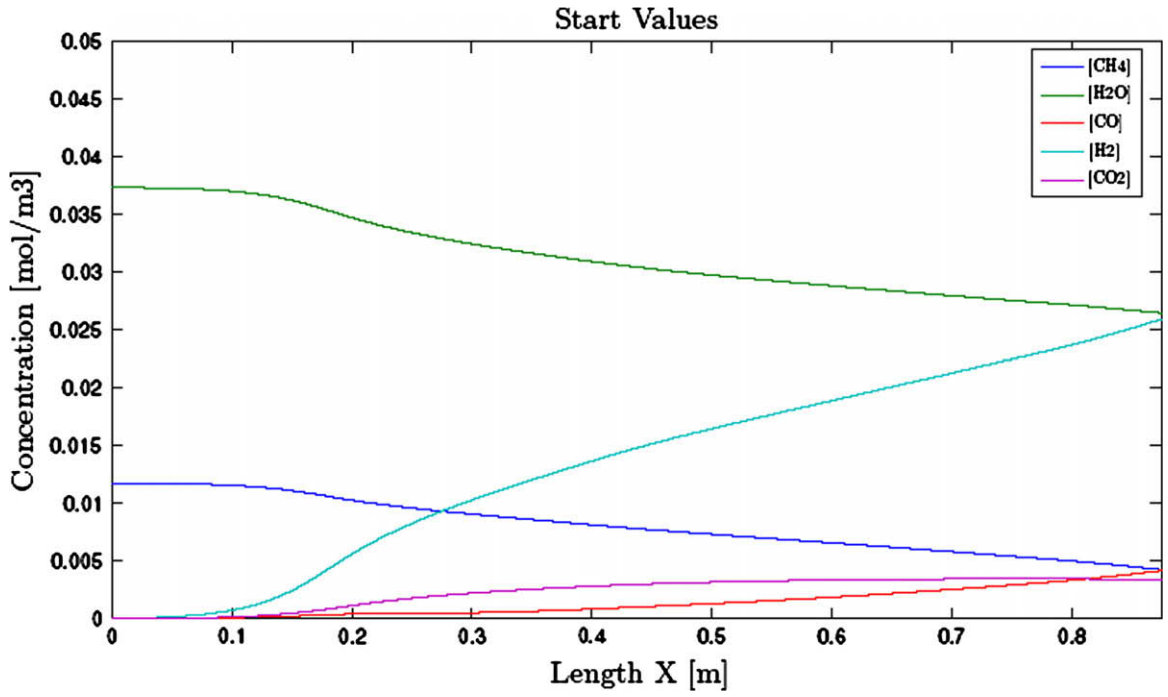

Fig. 5 – Calculated concentrations of reactants and products in the reformer as a function of distance of entrance.

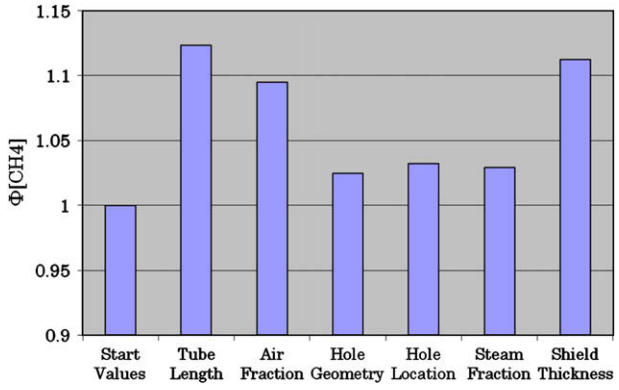

Fig. 6 – Conversion efficiency of methane to hydrogen by a change of 50% of six different design modifications. (1) Tube length, (2) air fraction, (3) hole geometry, (4) hole location, (5) steam fraction and (6) shield thickness. Results are normalized to a reference reformer mentioned 'Start Values'.

To start with, the increase in temperature of the tube happens everywhere except for at the end of the insulating shield. The second effect is comparable; an improved insulation at the end of the tube allows the burner to use more fuel which forces a higher temperature at the other parts of the reactor tube.

7. Conclusions

A fast and accurate model of a reformer has been developed by which several design modifications can be evaluated.

It is found that up to 9.5% more hydrogen can be produced by increasing the air fraction in the burner fuel by 50%, which requires minimal modification impact. More modification impact requires the increasing the thickness of the insulating shield by 50%, which results in 11.2% more hydrogen production. Besides this, this modification results in a desirable increase in heat distribution between the reactor tubes.

Apart from the technical optimization of a reformer, the feasibility of the improvements proposed still have to be investigated while taking in account costs and aspects related to production of the installation. However, our first results indicate that the application of analytical modeling in the design phase of a project can have beneficial effects on the final performance of an apparatus.

REFERENCES

[1] Seo Yong-Seog, Seo Dong-Joo, Seo Yu-Taek, Yoon Wang-Lai. Investigation of the characteristics of a compact steam reformer integrated with a water–gas shift reactor. J Power Sources 2006;161(2):1208–16.
[2] Bottino A, Comite A, Capannelli G, Felicedi R, Pinacci P. Steam reforming of methane in equilibrium membrane reactors for integration in power cycles. Catalysis Today 2006;118:214–22.
[3] Assaf EM, Jesus CDF, Assaf JM. Mathematical modelling of methane steam reforming in a membrane reactor: an isothermic model. Braz J Chem Eng 1998;15.
[4] Yeh GJ. Steam reforming program. Report Saudi Aramco, Dharan, Saudi Arabia; 2002.
[5] Barrio VL, Schaub G, Rohde M, Rabe S, Vogel F, Cambra JF, et al. Reactor modeling to simulate catalytic

partial oxidation and steam reforming of methane. Comparison of temperature profiles and strategies for hot spot minimization. Int J Hydrogen Energy 2007;32: 1421–8.
[6] Hulteberg PC, Burford H, Duraiswamy K, Porter B, Woods R. A cost effective steam reformer for a distributed hydrogen infrastructure. Int J Hydrogen Energy 2007;33:1266–74.
[7] Lutz Andrew E, Bradshaw Robert W, Keller Jay O, Witmer Dennis E. Thermodynamic analysis of hydrogen production by steam reforming. Int J Hydrogen Energy 2003; 28:159–67.
[8] Perry RP, Green DW. Perry's chemical engineers' handbook. The McGraw-Hill Companies Inc.; 1997.
[9] Scott Fogler H. Elements of chemical reaction engineering. Prentice-Hall International, Inc; 1999.
[10] Ryden M, Lyngfelt A. Using steam reforming to produce hydrogen with carbon dioxide capture by chemical-looping combustion. Int J Hydrogen Energy 2006;31(10):1271–83.
[11] Bird RB, Stewart WE. Transport phenomena. John Wiley & Sons; 2006.
[12] Sieder EN, Tate GE. Heat transfer and pressure drop of liquids in tubes. Ind Eng Chem 1936;28:1429–35.